HHS Public Access

Author manuscript

AJNR Am J Neuroradiol. Author manuscript; available in PMC 2017 March 01.

Published in final edited form as:

AJNR Am J Neuroradiol. 2016 September ; 37(9): 1643–1649. doi:10.3174/ajnr.A4836.

Differentiation of Low- and High-Grade Gliomas Using High b-Value Diffusion Imaging with A non-Gaussian Diffusion Model

Yi Sui[1,2,†], **Ying Xiong**[1,3,†], **Jingjing Jiang**[3], **M. Muge Karaman**[1], **Karin L. Xie**[4], **Wenzhen Zhu**[3,*], and **Xiaohong Joe Zhou**[1,2,4,5,*]

[1]Center for MR Research, University of Illinois at Chicago, Chicago, IL, USA

[2]Department of Bioengineering, University of Illinois at Chicago, Chicago, IL, USA

[3]Department of Radiology, Tongji Hospital, Tongji Medical College, Huazhong University of Science and Technology, Wuhan, Hubei, China

[4]Department of Radiology, University of Illinois at Chicago, Chicago, IL, USA

[5]Department of Neurosurgery, University of Illinois at Chicago, Chicago, IL, USA

Abstract

Background and Purpose—Imaging-based tumor grading is highly desirable, but faces challenges in sensitivity, specificity, or diagnostic accuracy. A recently proposed diffusion imaging method using a fractional order calculus (FROC) model offers a set of new parameters to probe not only the diffusion process itself, but also intra-voxel tissue structures, providing new opportunities for non-invasive tumor grading. This study aims at demonstrating the feasibility of using the FROC model to differentiate low- from high-grade gliomas in adult patients and illustrating its improved performance over a conventional diffusion imaging method employing ADC (or *D*).

Materials and Methods—With approval from the institutional review board (IRB) and written informed consents from all participating patients, 54 adult patients (18–70 years old) with histology-proven gliomas were enrolled and divided into a low-grade (n = 24) and a high-grade group (n = 30). Multi-b-value diffusion MRI was acquired with 17 b-values (0–4000s/mm^2) and analyzed using a FROC model. Mean values and standard deviations of three FROC parameters (*D*, β, and μ) were calculated from the normal contralateral thalamus (NCTH; as control) and the tumors, respectively. Based on these values, the low- and high-grade glioma groups were compared using a Mann-Whitney U-test. Receiver operating characteristic (ROC) analysis was performed to assess the performance of individual parameters as well as the combination of multiple parameters for low- versus high-grade differentiation.

[*]*Correspondence should be addressed to:* Xiaohong Joe Zhou, PhD, Advanced Imaging Center, Suite 103, 2242 West Harrison Street, Chicago, IL 60612, USA. Tel: +1 312-413-3979 (O), +1 312-355-1637 (FAX), xjzhou@uic.edu, Wenzhen Zhu, MD, Department of Radiology, Tongji Hospital, 1095 Jiefang Ave, Wuhan, Hubei 430030, China. Tel: +86 27-83663258 (O), zhuwenzhen@hotmail.com.
[†]These individuals contributed equally and share the first-authorship.

Presentation:
This work was presented in part at the 100th Annual Meeting of the RSNA.

Results—Each of the three FROC parameters exhibited a statistically higher value ($p \leq 0.011$) in the low-grade than in the high-grade gliomas, whereas there was no difference in the NCTH ($p \geq 0.706$). The ROC analysis showed that β (AUC = 0.853) produced a higher AUC than D (0.781) or μ (0.703), and offered a sensitivity of 87.5%, specificity of 76.7%, and diagnostic accuracy of 82.1%.

Conclusion—The study has demonstrated the feasibility of using a non-Gaussian FROC diffusion model to differentiate low- and high-grade gliomas. While all three FROC parameters showed statistically significant differences between the two groups, β exhibited better performance than the other two parameters, including ADC (or D).

Introduction

Gliomas are the most common primary brain tumors seen in adults, accounting for approximately one third to one half of all cases diagnosed[1] and 82% of malignant brain tumors[2]. According to the latest classification by the World Health Organization (WHO), gliomas can be divided into four grades, spanning a broad spectrum of biological aggressiveness[3]. Accurate grading of gliomas is pivotal in patient management, not only for selecting the most effective therapy for malignant tumors but also for avoiding unnecessary aggressive treatment for low-grade tumors prior to malignant transformation, maximizing the quality of life for the patients.

MRI has been widely used for initial diagnosis of brain tumors. Its role for tumor grading, however, is less established[4]. Conventional MRI techniques, including pre-contrast T1-weighted (T1W), T2-weighted (T2W), T2W FLAIR, and post-contrast T1W imaging, have limited sensitivity (e.g., 72.5%) and specificity (e.g., 65.0%) for differentiating low-from high-grade gliomas[4, 5]. Perfusion imaging (e.g., CBV) can improve the sensitivity to > 90%[6], but the specificity (e.g., 57.5%) remains inadequate and is subject to the choice of CBV threshold values depending on tumor types[7–9]. With the ability to reveal tumor metabolic changes, MRS has also been used for tumor grading[6, 10, 11]. The long data acquisition times, poor spatial resolution, and magnetic susceptibility perturbations at specific locations (e.g., near the sinus and the skull) have hindered its widespread clinical application[6, 10, 11]. Because of the aforementioned challenges and limitations faced by MRI/MRS, tissue biopsy remains to be the gold standard for tumor classification and grading, despite its sampling errors, invasiveness, and inability to evaluate residual tumor tissue after cytoreductive surgery[5].

Over the past two decades, diffusion imaging based on ADC has been evaluated for tumor grading[12–14]. Despite the potential, several studies indicate that ADC values overlap considerably among different tumor grades in both adult[15–17] and pediatric patients[14, 18–20]. The ADC values of tumor tissues are obtained by characterizing the diffusion MRI signals with a mono-exponential function, also known as a Gaussian diffusion model, which assumes that the diffusion process within a voxel is homogeneous[21]. Unlike low-grade gliomas, high-grade gliomas are hallmarked with an increased degree of tissue heterogeneity[22, 23], which is not adequately captured by ADC. To overcome this limitation, a number of non-Gaussian diffusion models[24–32] have been developed to extract tissue

microstructural information, including tissue heterogeneity, beyond what ADC can provide. The fractional order calculus (FROC) model[26, 29], for example, can produce a set of parameters, including diffusion coefficient D (in $\mu m^2/ms$), fractional order derivative in space β, and a spatial parameter μ (in μm). These parameters provide additional avenues to probing not only the diffusion process itself (D), but also the intra-voxel tissue heterogeneity (β) that can be used to improve tumor characterization[26, 29, 33]. In this study, we demonstrate the feasibility of using a new set of parameters from the FROC model to improve MR-based differentiation of low- and high-grade gliomas in adult patients.

Materials and Methods

Patients

The institutional review board (IRB) of the performing hospital approved this prospective study and the written informed consents were obtained from all participating patients. Fifty-six adult patients (18–70 years old) with initial diagnosis of gliomas were recruited, and underwent multi-b-value diffusion MRI prior to biopsy or surgical treatment. Two patients were excluded from the analysis due to excessive motion. Among the 54 patients included in the study, histopathology revealed 24 low-grade gliomas including 1 pilocytic astrocytoma (WHO I), 2 oligodendroglioma (WHO I and II), 20 astrocytoma (WHO II; predominantly diffuse tumors), and 1 ganglioglioma (WHO II), and 30 high-grade gliomas including 2 anaplastic oligodendroglioma (WHO III), 10 anaplastic astrocytoma (WHO III), and 18 glioblastoma multiforme (GBM; WHO IV), according to the WHO guideline of 2007[3].

Image Acquisition

All MRI examinations were performed on a 3 Tesla scanner (MR750; General Electric Healthcare, Milwaukee, WI) with a 32-channel phased-array head coil. The imaging protocol included pre-contrast T1W FLAIR, T2W FLAIR, T2W PROPELLER, and multi-b-value diffusion-weighted (DW) sequences, followed by post-contrast T1W imaging. Susceptibility-weighted imaging was applied on selected patients when the conventional sequences were inadequate to characterize hemorrhage within tumors. In all sequences, a FOV of 24cm and a slice thickness of 5mm were used. The parameters specific to each anatomic imaging sequence were: T1W FLAIR: TR/TE = 1750/32.4 ms, TI = 860 ms, flip angle = 90°, and matrix size = 320×320; T2W PROPELLER: TR/TE = 4260/102 ms, echo train length = 32, and matrix size = 320×224; T2W FLAIR: TR/TE = 8400/150 ms, TI = 2100 ms, echo train length = 26, and matrix size = 256×256. The DW images were produced using a single-shot echo-planar imaging (EPI) sequence with 17 b-values (0_1, 20_1, 50_1, 100_1, 200_1, 400_1, 600_1, 800_1, 1000_1, 1200_1, 1600_1, 2000_2, 2400_2, 2800_2, 3200_4, 3600_4 and 4000_4 s/mm^2, where the subscript denotes the number of averages). At each b-value, a Stejskal-Tanner diffusion gradient was successively applied along the x-, y-, and z-axis to obtain a trace-weighted image in order to minimize the influence of diffusion anisotropy. The key data acquisition parameters were TR/TE = 3025/94.5 ms, SENSE acceleration factor = 2, separation between two diffusion gradient lobes Δ = 38.6 ms, duration of each diffusion gradient δ = 32.2 ms, matrix size = 160×160 (reconstructed with a 256×256 matrix), and the scan time = 4.5 minutes.

Image Analysis

Equation [1] was used to fit the intensity (S) of the multi-b-value diffusion images voxel-by-voxel, according to the FROC diffusion model[26, 29]:

$$S=S_0\exp\left[-D\mu^{2(\beta-1)}(\gamma G_d\delta)^{2\beta}\left(\Delta-\frac{2\beta-1}{2\beta+1}\delta\right)\right]. \quad [1]$$

where S_0 is the signal intensity without diffusion weighting, G_d is the diffusion gradient amplitude, and δ and Δ are defined earlier. The β parameter (dimensionless; $0<\beta\leq1$) is a fractional order derivative with respect to space, and μ (in units of μm) is a spatial constant to preserve the nominal units of diffusion coefficient D (in mm^2/s). In the fitting, D (which reflects the intrinsic diffusivity) was estimated by a mono-exponential model using the data acquired at lower b-values (≤ 1000 sec/mm^2), in an attempt to make D equivalent to conventional ADC. After D was determined, β and μ were subsequently obtained from a voxel-wise non-linear fitting using a Levenberg-Marquardt algorithm[34] with all b-values.

Regions of interest (ROIs) were first placed on the normal contralateral thalamus (NCTH), which served as an internal control, followed by placing ROIs on the solid region of tumors by two neuro-radiologists (Y.X. and K.X. with 8 years and 15 years of clinical experience, respectively) blinded to the histology grades. Guided by the high-resolution anatomic images, regions of hemorrhage, cystic change and/or necrosis were excluded. In the solid region of tumors, the enhancing components and the non-enhancing (or not-so-obvious enhancing) components were measured and averaged. The ROI-based image analysis was performed with customized software developed in MATLAB (MathWorks, Inc., Natick, MA).

Statistical Analysis

Mean and standard deviation of D, β, and μ for each patient were calculated from the NCTH and the tumor ROIs, respectively. Based on these values, the low-grade and high-grade glioma groups were compared using a Mann-Whitney U-test with a statistical significance set at $p < 0.05$.

To investigate the potential value of using combinations of the FROC parameters (D, β, and μ) for differentiation of low- and high-grade gliomas, a logistic regression model was attempted:

$$P_0=\exp(a_0+a_1D+a_2\beta+a_3\mu)/[1+\exp(a_0+a_1D+a_2\beta+a_3\mu)] \quad [2]$$

where a_0 is a constant, a_1, a_2, and a_3 are the regression coefficients for D, β, and μ, respectively. The regression coefficients were estimated using a maximum likelihood method[35]. Receiver operating characteristic (ROC) analysis was performed to determine the area under the ROC curve (AUC) for assessing the performance of tumor differentiation using each of the three FROC parameters individually as well as the combination of FROC parameters represented by P_0. The best cutoff values in the ROC analysis were determined

using Youden's index. To determine the generalizability of the proposed method, a holdout cross-validation algorithm was employed by applying the logistic regression model in Eq. [2] on a "training dataset" and a "test dataset" (randomly and equally split from the samples). The Pearson's correlation coefficients were then determined between the predicted values and the "true" histopathological results. All statistical analyses were carried out using SPSS software (SPSS, Inc., Chicago, IL).

Results

Comparison between Representative Patients in Each Group

Figure 1 shows a set of axial images from a representative patient (oligodendroglioma WHO I) in the low-grade glioma group, including T2W EPI (Fig. 1a), and the FROC maps (color images in Fig. 1b–d). The pre-contrast and post-contrast T1W FLAIR, pre-contrast T2W FLAIR, and T2W PROPELLER images are available online (Fig. A). The D, β, and μ maps (Figs. 1b–d, respectively) all exhibited higher values in the tumor than in the surrounding brain parenchyma. Figure 2 shows a set of axial images from a representative patient (GBM, WHO IV) in the high-grade glioma group using a layout similar to that of Fig. 1. The FROC parameters D, β, and μ (Figs. 2b–d, respectively) were considerably lower compared to those in Figs. 1b–d, leading to a distinct difference between the high- and low-grade tumors. Additional anatomic images are available online (Fig B).

Group Comparison based on the FROC Parameters

After calculating the mean values of the FROC parameters from each tumor ROI, the means and standard deviations from each patient group were obtained and listed in Table 1. Since D is mathematically equivalent to the conventional ADC (see Materials and Methods), an agreement of >96% was observed between D from the FROC model and ADC from a mono-exponential fitting using two b-values (b = 0 and 1000 sec/mm^2), as typically done in clinical studies. Thus, ADC and D are used interchangeably in this study. Comparison of the FROC parameters between the two tumor groups is shown in a set of box plots (Fig. 3). Consistent with the representative cases in Figs. 1 and 2, the group analysis exhibited statistically higher values ($p \leq 0.011$) in the low-grade than the high-grade gliomas for each of the three FROC parameters. In comparison, the internal control using NCTH showed no significant differences ($p \geq 0.706$) in the FROC parameters between the two patient groups, as summarized in Table 1.

ROC Analysis

Figure 4 illustrates the ROC curves of using individual FROC parameters for differentiating low- (positive) from high-grade (negative) gliomas. Since D and μ were strongly correlated (see the results below in Fig. 5), μ was excluded from the logistic regression to avoid over weighting. The constant and regression coefficients of D and β were 19.936, −0.012, and −24.145, respectively (see Eq. [2]), and the corresponding P_0 was used in ROC analysis to represent the combination of D and β. Table 2 summarizes the cutoff values with the corresponding sensitivity, specificity, accuracy, the positive and negative predicted values (PPV and NPV), and asymptotic significance (p-value). Although D offered the highest sensitivity (91.7%), its specificity was the lowest (63.3%), leading to a moderate accuracy

(77.5%). The sensitivity was noticeably improved by β or the combination of β and *D*, which resulted in the best accuracy (82.1%). The AUC values of the ROC analyses together with their 95% confidence intervals (CIs) and standard errors (SEs) are given in Table 3. The parameter β had a higher AUC (0.853) than *D* (0.781) or μ (0.703), indicating a better performance for glioma differentiation. It is worth noting that the combination of *D* and β did not improve the sensitivity, specificity, accuracy and AUC when compared with β.

The cross-validation analysis showed that the Pearson's correlation coefficients between the predicted values and the "true" histopathological results were 0.529 (*p*-value < 0.01) for the training set and 0.625 (*p*-value < 0.01) for the test set. The significance test for the difference between the two correlations (Fisher's *z*-test) resulted in a *p*-value of 0.617, suggesting that the training and test datasets did not produce statistically different correlations.

The scatter plots in Fig. 5 illustrate the possible (or lack of) correlation between the FROC parameters using all patient data. A very strong correlation between *D* and μ was observed (Fig. 5a) with a Pearson's correlation coefficient of r = 0.930 ($p < 0.001$). In contrast, a noticeably weaker correlation was seen between *D* and β (r = 0.766 $p < 0.001$). In Fig. 5b, the best cutoff values of *D* and β are indicated by the vertical (red) and the horizontal (green) lines, respectively. The diagonal black line in Fig. 5b corresponds to the cutoff probability of $P_0 = 0.662$ for the combination of *D* and β. The close proximity between the black and green lines is a reflection that *D* has a considerably smaller role than β in the equation $P_0 = \exp(19.936 - 0.012D - 24.145\beta) / [1 + \exp(19.936 - 0.012D - 24.145\beta)]$.

Discussion

We have investigated the feasibility of using a set of novel FROC diffusion parameters to differentiate low- from high-grade gliomas in adults and demonstrated that *D*, β, and μ exhibited significant differences between the two tumor groups. When used individually, β outperformed the other two parameters. These results are important as they demonstrate that new parameters from the FROC diffusion model can contribute positively to glioma differentiation and extend the capability of diffusion imaging beyond conventional ADC.

Over the past two decades, ADC has been applied to differentiating a number of brain tumors[14, 16, 18, 36], including gliomas. Although the sensitivity of using ADC to detect neoplastic changes has been demonstrated, it is well known that considerable overlap in ADC values exists between low- and high-grade brain tumors[14, 16, 17], compromising the specificity and diagnostic accuracy. The sub-optimal performance of ADC for tumor grading originates, at least in part, from the use of a Gaussian diffusion model (i.e., the mono-exponential model) which assumes a homogeneous diffusion process in tumor, despite overwhelming evidence of tumor heterogeneity[37–39]. In the presence of heterogeneity, non-Gaussian diffusion models can be more effective in characterizing the complex diffusion process, particularly at high b-values (e.g., $b \geq 1500$ s/mm^2)[15, 21–32, 36, 40].

Like other non-Gaussian diffusion models, the FROC diffusion model provides new parameters complementary to ADC. In the FROC model, correlation between β and intra-voxel tissue heterogeneity has been suggested in several studies on phantoms and tissue

specimens[26, 29, 41, 42]. This correlation is also supported by *in vivo* studies indicating that tissues with a smaller β value exhibit a larger degree of intra-voxel heterogeneity[22, 27, 33, 43]. It is interesting to note that tissue heterogeneity is also a contributing factor to the WHO tumor grading system[44]. Thus, β parameter may provide a link between an MR measurement and WHO grades. The lower β values (i.e., high degree of intra-voxel heterogeneity) seen in high-grade gliomas (Figs. 2 and 3) are consistent with the increased degree of tissue heterogeneity because of the presence of edema, necrosis, hemorrhage, micro-calcification, etc. This observation is also consistent with a recent study on pediatric brain tumors[33, 43] in which high grade tumors showed significantly lower β value compared to their low-grade counterpart. Further studies on well-controlled excised tissues are needed to directly establish and validate the correlation between diffusion heterogeneity suggested by β and structural heterogeneity revealed by histopathology.

Kwee et al. recently studied high-grade gliomas[27] using an alternative non-Gaussian diffusion model based on a stretched-exponential formulism[28]. Although this model is similar to the FROC model, the stretched-exponential is developed empirically instead of using fractionalized Fick's diffusion equation. The heterogeneity index α in the stretched-exponential model resembles to β in this study. The α value for high-grade gliomas was reported to be 0.58 ± 0.08, which is lower than $\beta = 0.77 \pm 0.06$ in our study. This is most likely due to the different diffusion times (Δ) employed in these studies[45]. Compared to the study of Kwee et al., our study produced a noticeably smaller standard deviation in β because of the relatively large number of b-values employed. Although a minimum of 4 b-values is needed to obtain the three FROC parameters, a larger number of b-values improve the robustness of the non-linear fitting, particularly when the signal-to-noise ratio (SNR) is low.

Using all the patient data in this study, a strong linear correlation was observed between D and μ (Fig. 5a). As μ has been related to the dimension of free diffusion space[26], the correlation in Fig. 5a reflects the classical relationship between diffusion rate and mean free length. It is interesting to note that β was less correlated with D or μ. This weaker correlation can be exploited to improve specificity and diagnostic accuracy, as these two parameters act more independently. In this study, we have seen a number of evidences suggesting β is a more dominant parameter than D for differentiating the low- from high-grade gliomas, as the combination of β with D did not significantly improve the performance compared to using D alone. This suggests the important role of tumor heterogeneity in various tumor grades.

Our study has several limitations. First, despite the improvement offered by the FROC model in glioma grading, the sensitivity, specificity, and diagnostic accuracy remain sub-optimal. An extension of the FROC model to capturing temporal heterogeneity, as demonstrated recently[42, 43], suggests new opportunities to further improve the performance. These non-Gaussian diffusion imaging techniques may eventually help complementing surgical biopsy in situations where tissue biopsy is difficult or risky. Second, the number of patients enrolled in the study is moderate. As such, we did not attempt to further distinguishing glioma sub-types or individual grades. Finally, limited by the SNR, the highest b-value attempted in this study was 4000 s/mm^2, although an even higher b-value may further improve reliability of extracting the FROC diffusion parameters[26, 29, 45].

Despite these limitations, we have demonstrated the feasibility of using high b-value diffusion MRI together with the FROC diffusion model to improve differentiation between low- and high-grade gliomas. In particular, the new parameter β offers a higher diagnostic accuracy than using diffusion coefficient (*D* or ADC) alone, and is the most useful and dominant parameter among the three FROC parameters for differentiating glioma grades. Although the focus of this study is on gliomas, the non-Gaussian diffusion imaging approach demonstrated herein is expected to have applications in other disease processes which involve tissue heterogeneity changes.

Supplementary Material

Refer to Web version on PubMed Central for supplementary material.

Acknowledgments

This work was supported in part by the National Natural Science Foundation of China (grant number: 81171308), the National Program of the Ministry of Science and Technology of China under the “12th Five-year Plan” (grant number: 2011BAI08B10), and the US National Institute of Health (grant number: 1S10RR028898). The authors are grateful to Drs. Keith R. Thulborn, Kejia Cai, and Frederick C. Damen for helpful discussions.

DISCLOSURES: Yi Sui—*UNRELATED: Employment:* GE Healthcare, Comments: Joined GE Healthcare after the work was done. **Xiaohong Joe Zhou—***RELATED: Grant:* NIH Grant; No. 1S10RR028898*; *UNRELATED: Consultancy:* Horizon Medical Physics Services, Comments: Consulting fees and ownership; *Grants/Grants Pending:* NIH Grant No. 1R21EB023050-01,* Abbvie Pharmaceuticals,* Comments: Federal or industrial grant support; *Royalties:* Elsevier Publishing, Comments: Royalty payment for a book I co-authored.

**money paid to institution*

References

1. Ostrom QT, Gittleman H, Liao P, et al. CBTRUS statistical report: primary brain and central nervous system tumors diagnosed in the United States in 2007–2011. Neuro Oncol. 2014; 16(Suppl 4):iv1–iv63. [PubMed: 25304271]
2. Omuro A, DeAngelis LM. Glioblastoma and other malignant gliomas: a clinical review. JAMA. 2013; 310:1842–1850. [PubMed: 24193082]
3. Louis DN, Ohgaki H, Wiestler OD, et al. The 2007 WHO classification of tumours of the central nervous system. Acta Neuropathol. 2007; 114:97–109. [PubMed: 17618441]
4. Upadhyay N, Waldman AD. Conventional MRI evaluation of gliomas. Br J Radiol. 2011; 84(Spec No 2):S107–S111. [PubMed: 22433821]
5. Law M, Yang S, Wang H, et al. Glioma grading: sensitivity, specificity, and predictive values of perfusion MR imaging and proton MR spectroscopic imaging compared with conventional MR imaging. AJNR Am J Neuroradiol. 2003; 24:1989–1998. [PubMed: 14625221]
6. Poussaint TY, Rodriguez D. Advanced neuroimaging of pediatric brain tumors: MR diffusion, MR perfusion, and MR spectroscopy. Neuroimaging Clin N Am. 2006; 16:169–192. [PubMed: 16543091]
7. Law M, Young RJ, Babb JS, et al. Gliomas: predicting time to progression or survival with cerebral blood volume measurements at dynamic susceptibility-weighted contrast-enhanced perfusion MR imaging. Radiology. 2008; 247:490–498. [PubMed: 18349315]
8. Young GS, Setayesh K. Spin-echo echo-planar perfusion MR imaging in the differential diagnosis of solitary enhancing brain lesions: distinguishing solitary metastases from primary glioma. AJNR Am J Neuroradiol. 2009; 30:575–577. [PubMed: 19095787]
9. Hirai T, Murakami R, Nakamura H, et al. Prognostic value of perfusion MR imaging of high-grade astrocytomas: long-term follow-up study. AJNR Am J Neuroradiol. 2008; 29:1505–1510. [PubMed: 18556364]

10. Schneider JF, Confort-Gouny S, Viola A, et al. Multiparametric differentiation of posterior fossa tumors in children using diffusion-weighted imaging and short echo-time 1H-MR spectroscopy. J Magn Reson Imaging. 2007; 26:1390–1398. [PubMed: 17968955]
11. Ishimaru H, Morikawa M, Iwanaga S, et al. Differentiation between high-grade glioma and metastatic brain tumor using single-voxel proton MR spectroscopy. Eur Radiol. 2001; 11:1784–1791. [PubMed: 11511902]
12. Kang Y, Choi SH, Kim YJ, et al. Gliomas: Histogram analysis of apparent diffusion coefficient maps with standard- or high-b-value diffusion-weighted MR imaging--correlation with tumor grade. Radiology. 2011; 261:882–890. [PubMed: 21969667]
13. Raab P, Hattingen E, Franz K, et al. Cerebral gliomas: diffusional kurtosis imaging analysis of microstructural differences. Radiology. 2010; 254:876–881. [PubMed: 20089718]
14. Rumboldt Z, Camacho DL, Lake D, et al. Apparent diffusion coefficients for differentiation of cerebellar tumors in children. AJNR Am J Neuroradiol. 2006; 27:1362–1369. [PubMed: 16775298]
15. Bian W, Khayal IS, Lupo JM, et al. Multiparametric characterization of grade 2 glioma subtypes using magnetic resonance spectroscopic, perfusion, and diffusion imaging. Transl Oncol. 2009; 2:271–280. [PubMed: 19956389]
16. Maier SE, Sun Y, Mulkern RV. Diffusion imaging of brain tumors. NMR Biomed. 2010; 23:849–864. [PubMed: 20886568]
17. Yamasaki F, Kurisu K, Satoh K, et al. Apparent diffusion coefficient of human brain tumors at MR imaging. Radiology. 2005; 235:985–991. [PubMed: 15833979]
18. Bull JG, Saunders DE, Clark CA. Discrimination of paediatric brain tumours using apparent diffusion coefficient histograms. Eur Radiol. 2012; 22:447–457. [PubMed: 21918916]
19. Poretti A, Meoded A, Huisman TA. Neuroimaging of pediatric posterior fossa tumors including review of the literature. J Magn Reson Imaging. 2012; 35:32–47. [PubMed: 21989968]
20. Porto L, Jurcoane A, Schwabe D, et al. Differentiation between high and low grade tumours in paediatric patients by using apparent diffusion coefficients. Eur J Paediatr Neurol. 2013; 17:302–307. [PubMed: 23273960]
21. Le Bihan D. The 'wet mind': water and functional neuroimaging. Phys Med Biol. 2007; 52:R57–R90. [PubMed: 17374909]
22. Pfister S, Hartmann C, Korshunov A. Histology and molecular pathology of pediatric brain tumors. J Child Neurol. 2009; 24:1375–1386. [PubMed: 19841426]
23. Gauvain KM, McKinstry RC, Mukherjee P, et al. Evaluating pediatric brain tumor cellularity with diffusion-tensor imaging. AJR Am J Roentgenol. 2001; 177:449–454. [PubMed: 11461881]
24. Le Bihan D. Intravoxel incoherent motion perfusion MR imaging: a wake-up call. Radiology. 2008; 249:748–752. [PubMed: 19011179]
25. Jensen JH, Helpern JA, Ramani A, et al. Diffusional kurtosis imaging: the quantification of non-gaussian water diffusion by means of magnetic resonance imaging. Magn Reson Med. 2005; 53:1432–1440. [PubMed: 15906300]
26. Magin RL, Abdullah O, Baleanu D, et al. Anomalous diffusion expressed through fractional order differential operators in the Bloch-Torrey equation. J Magn Reson. 2008; 190:255–270. [PubMed: 18065249]
27. Kwee TC, Galban CJ, Tsien C, et al. Intravoxel water diffusion heterogeneity imaging of human high-grade gliomas. NMR Biomed. 2010; 23:179–187. [PubMed: 19777501]
28. Bennett KM, Schmainda KM, Bennett RT, et al. Characterization of continuously distributed cortical water diffusion rates with a stretched-exponential model. Magn Reson Med. 2003; 50:727–734. [PubMed: 14523958]
29. Zhou XJ, Gao Q, Abdullah O, et al. Studies of anomalous diffusion in the human brain using fractional order calculus. Magn Reson Med. 2010; 63:562–569. [PubMed: 20187164]
30. Ozarslan E, Basser PJ, Shepherd TM, et al. Observation of anomalous diffusion in excised tissue by characterizing the diffusion-time dependence of the MR signal. J Magn Reson. 2006; 183:315–323. [PubMed: 16962801]
31. Yablonskiy DA, Bretthorst GL, Ackerman JJ. Statistical model for diffusion attenuated MR signal. Magn Reson Med. 2003; 50:664–669. [PubMed: 14523949]

32. Bar-Shir A, Cohen Y. High b-value q-space diffusion MRS of nerves: structural information and comparison with histological evidence. NMR Biomed. 2008; 21:165–174. [PubMed: 17492659]
33. Sui Y, Wang H, Liu G, et al. Differentiation of Low- and High-Grade Pediatric Brain Tumors with High b-Value Diffusion-weighted MR Imaging and a Fractional Order Calculus Model. Radiology. 2015; 277:489–496. [PubMed: 26035586]
34. Press, WH.; Teukolsky, SA.; Vetterling, WT.; Flannery, BP. Numerical Recipes 3rd Edition: The Art of Scientific Computing. New York: Cambridge University Press; 2007. p. 1262
35. Menard, S. Applied Logistic Regression Analysis. Thousand Oaks: SAGE; 2002. p. 1-120.
36. Khayal IS, McKnight TR, McGue C, et al. Apparent diffusion coefficient and fractional anisotropy of newly diagnosed grade II gliomas. NMR Biomed. 2009; 22:449–455. [PubMed: 19125391]
37. Janiszewska M, Beca F, Polyak K. Tumor heterogeneity: the Lernaean hydra of oncology? Oncology (Williston Park). 2014; 28:781–782. 784. [PubMed: 25224477]
38. Burrell RA, McGranahan N, Bartek J, et al. The causes and consequences of genetic heterogeneity in cancer evolution. Nature. 2013; 501:338–345. [PubMed: 24048066]
39. Marusyk A, Almendro V, Polyak K. Intra-tumour heterogeneity: a looking glass for cancer? Nat Rev Cancer. 2012; 12:323–334. [PubMed: 22513401]
40. Grinberg F, Farrher E, Kaffanke J, et al. Non-Gaussian diffusion in human brain tissue at high b-factors as examined by a combined diffusion kurtosis and biexponential diffusion tensor analysis. Neuroimage. 2011; 57:1087–1102. [PubMed: 21596141]
41. Magin RL, Akpa BS, Neuberger T, et al. Fractional Order Analysis of Sephadex Gel Structures: NMR Measurements Reflecting Anomalous Diffusion. Commun Nonlinear Sci Numer Simul. 2011; 16:4581–4587. [PubMed: 21804746]
42. Ingo C, Magin RL, Colon-Perez L, et al. On random walks and entropy in diffusion-weighted magnetic resonance imaging studies of neural tissue. Magn Reson Med. 2014; 71:617–627. [PubMed: 23508765]
43. Karaman MM, Sui Y, Wang H, et al. Differentiating low- and high-grade pediatric brain tumors using a continuous-time random-walk diffusion model at high b-values. Magn Reson Med. 2015
44. Rosenblum MK. The 2007 WHO Classification of Nervous System Tumors: newly recognized members of the mixed glioneuronal group. Brain Pathol. 2007; 17:308–313. [PubMed: 17598823]
45. Zhou, XJ.; Gao, Q.; Sirinivasan, G., et al. Dependence of Fractional Order Diffusion Model Parameters on Diffusion Time. Proc. of the 17th Annual Meeting of the International Society for Magnetic Resonance in Medicine; Honolulu, Hawai'i. April 18–24, 2009;
46. DeLong ER, DeLong DM, Clarke-Pearson DL. Comparing the areas under two or more correlated receiver operating characteristic curves: a nonparametric approach. Biometrics. 1988; 44:837–845. [PubMed: 3203132]

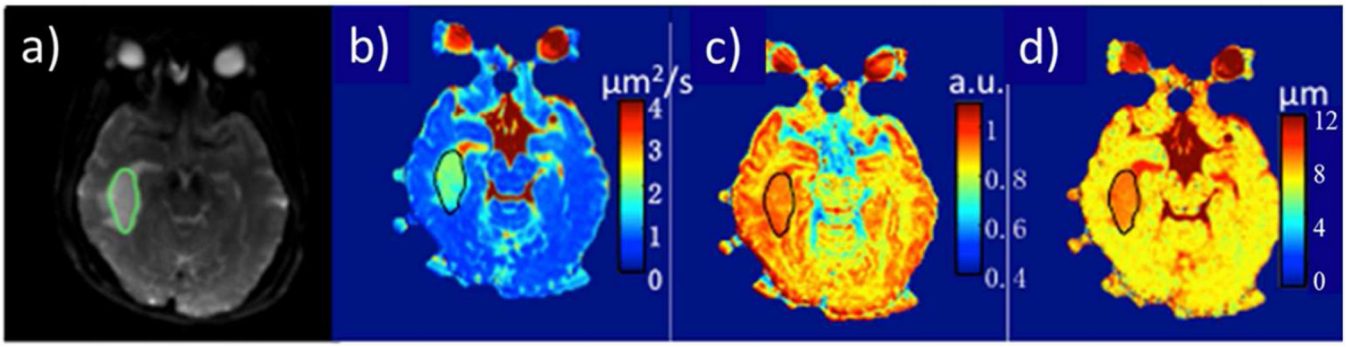

Figure 1.

A 41 years-old female patient with a low-grade glioma (oligodendroglioma, WHO grade I). T2W EPI at b = 0 with the tumor ROI encircled in green (a), and FROC parameter maps of *D* (b), β (c), and μ (d) with the tumor ROIs indicated by the black contours (see online Figure A for a complete set of images including axial pre-contrast T1W FLAIR (e), post-contrast T1W FLAIR (f), pre-contrast T2W FLAIR (g), and pre-contrastT2W PROPELLER (h) images). Compared to the GBM patient in Fig. 2, all three FROC parameters exhibited higher values.

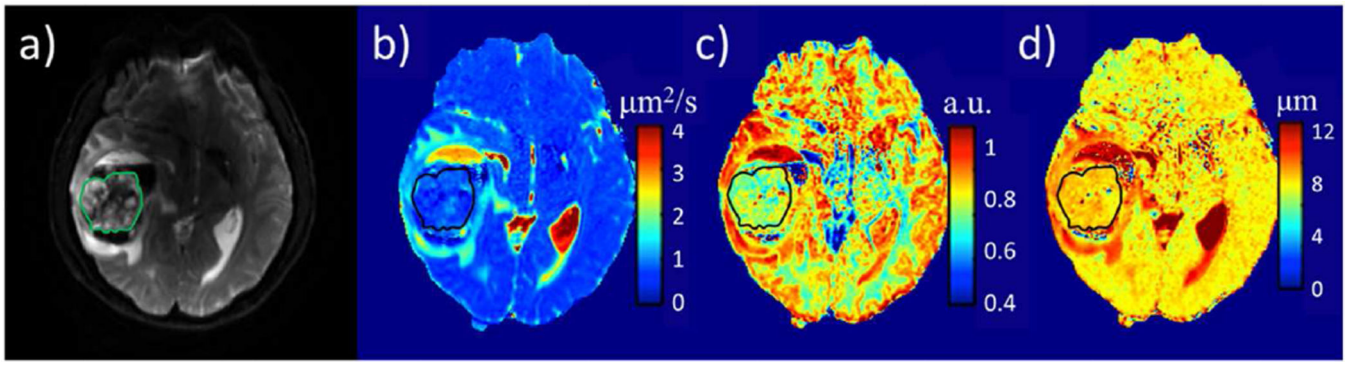

Figure 2.

A 38 years-old male patient with a high-grade glioma (GBM, WHO grade IV). T2W EPI at b=0 with the tumor ROI encircled in green (a), and FROC parameter maps of D (b), β (c), and μ (d) with the tumor ROIs indicated by the black contours (see online Figure B for a complete set of images including axial pre-contrast T1W FLAIR (e), post-contrast T1W FLAIR (f), T2W FLAIR (g), and T2W PROPELLER (h) images). Compared to the oligodendroglioma patient in Fig. 1, all three FROC parameters exhibited lower values.

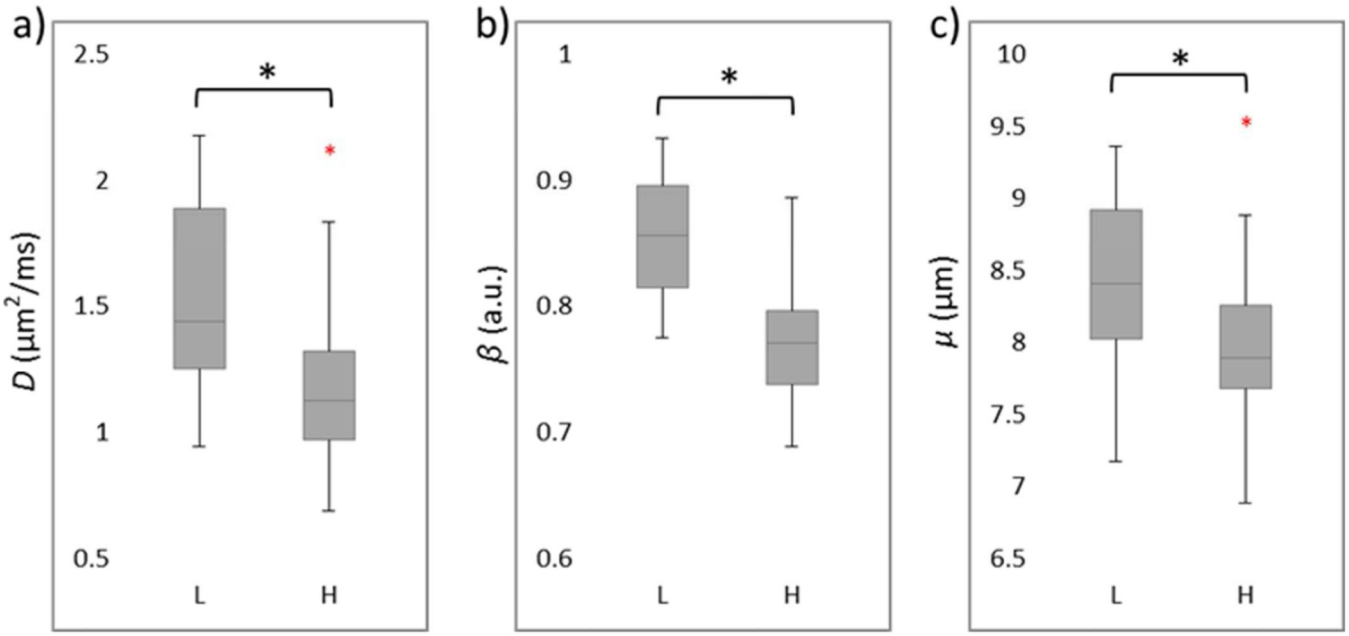

Figure 3.

Box plots of FROC parameters *D* (a), β (b), and μ (c) between the low- (L) and high-grade (H) gliomas. Boxes represent the 25th and 75th percentiles with the median indicated by the middle line in the box. Vertical end bars denote the range of data except for the outliers (i.e., values larger than the 75th percentile or smaller than the 25th percentile) represented by red +. The asterisk (*) indicates a significant difference ($p < 0.05$) between the low- and high-grade gliomas.

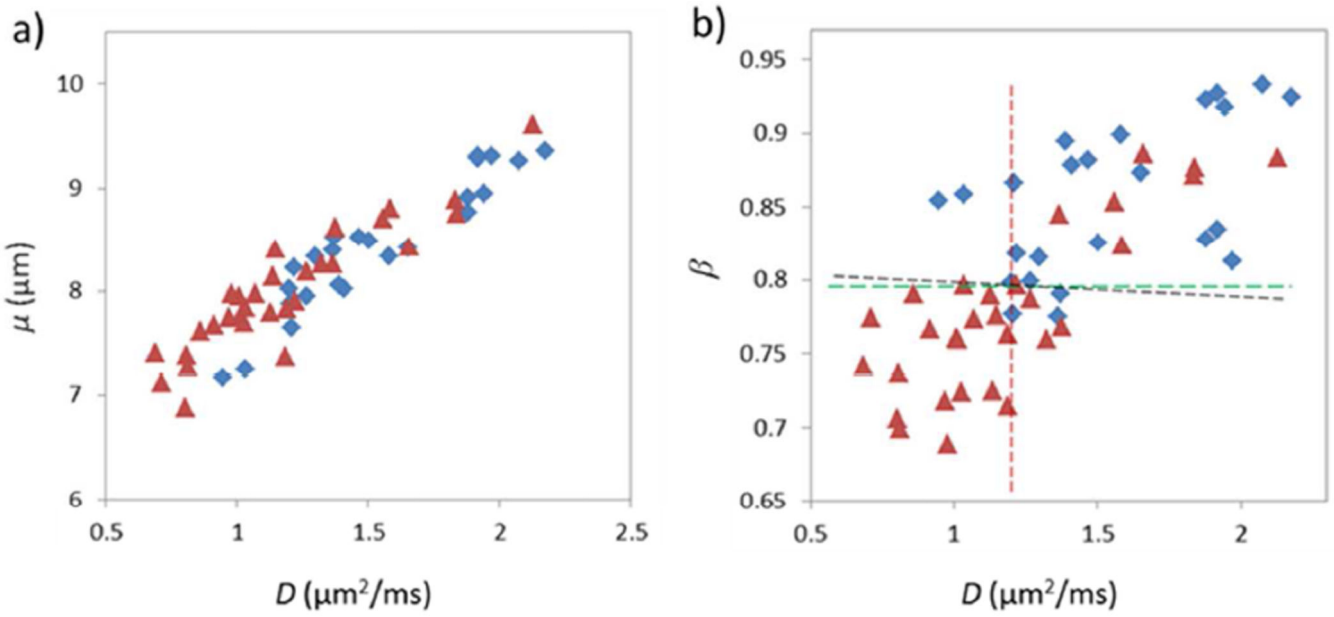

Figure 4.

ROC curves for β (in red), *D* (in green), μ (in blue) for differentiating between low- and high-grade gliomas. The diagonal line serves as a reference.

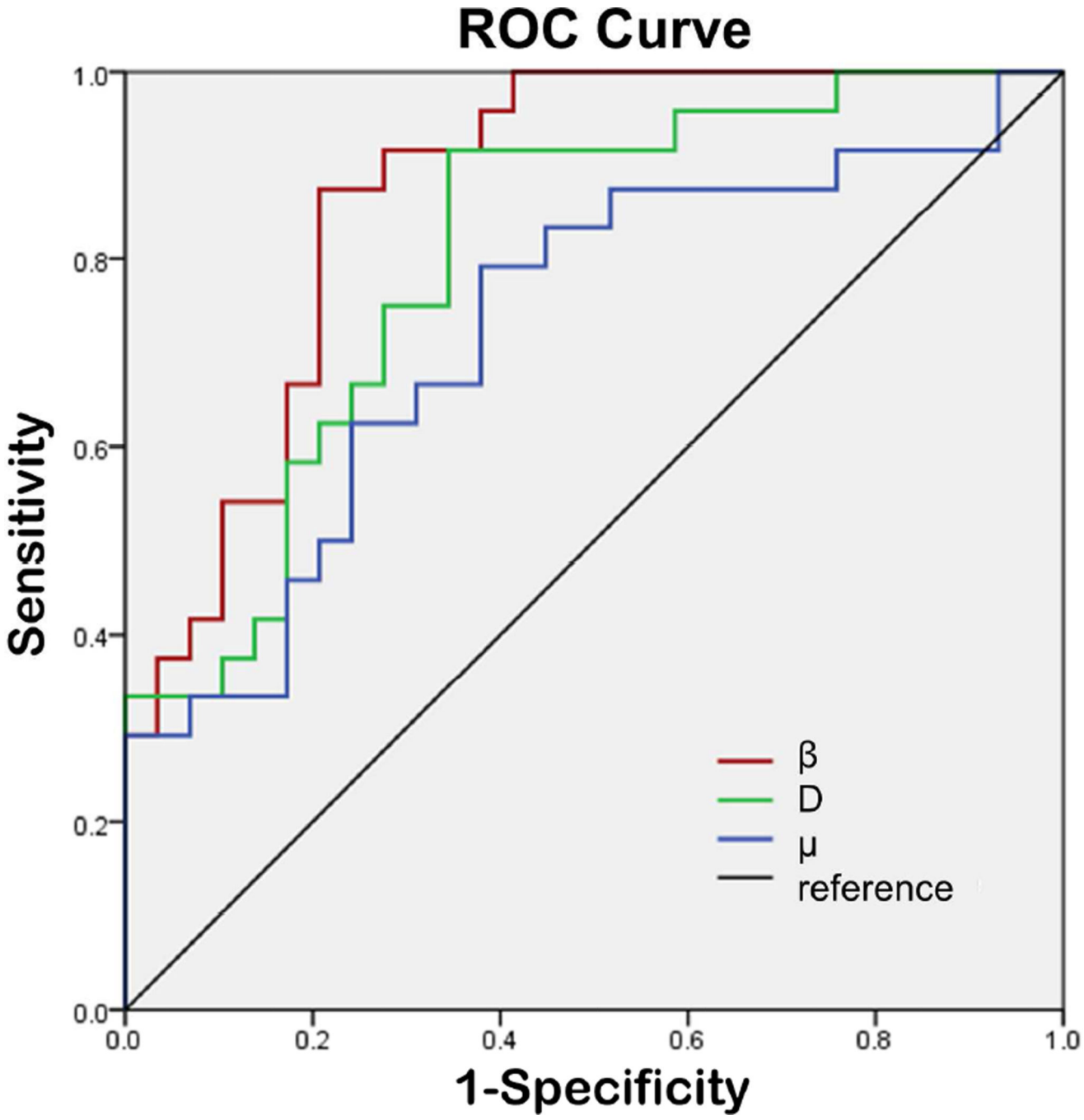

Figure 5.

Scatter plots of *D* vs. μ (a) and *D* vs. β (b) from all patients (the blue diamonds represent low grade and the red triangles denote high grade). A very strong correlation between *D* and μ (a) (Pearson's correlation coefficient r = 0.930; $p < 0.001$) and a weaker correlation between *D* and β (b) (Pearson's correlation coefficient r = 0.766; $p < 0.001$) are illustrated. The dashed lines in (b) indicate the cutoff values for *D* (red), β (green), and the combination of *D* and β (black; linear equation: $\beta = 0.000497D + 0.798$)

Table 1

FROC parameters of gliomas and normal contralateral thalamus (NCTH) of patients with low-grade (LG) and high-grade (HG) gliomas.

		D (μm²/ms)	β	μ (μm)
Gliomas	LG	1.54±0.35	0.85±0.05	8.43±0.63
	HG	1.19±0.36	0.77±0.06	8.01±0.59
	p-value *	<0.001	<0.001	0.011
NCTH	LG	0.76±0.06	0.78±0.03	7.33±0.38
	HG	0.76±0.04	0.78±0.03	7.34±0.33
	p-value *	0.876	0.706	0.890

* Mann-Whitney U-test

Table 2

*Cutoff, sensitivity, specificity, diagnostic accuracy, and asymptotic significance (*p*-value) using *D*, β, μ, and combination of *D* and β for differentiating low- (positive) from high-grade (negative) gliomas.

	Cutoff	Sensitivity	Specificity	Accuracy	PPV	NPV	*p*-value
D	1.189	91.7%	63.3%	77.5%	66.7%	90.5%	<0.001
β	0.797	87.5%	76.7%	82.1%	75.0%	88.5%	<0.001
μ	7.969	79.2%	60.0%	69.6%	61.3%	78.3%	0.0059
***D*+ β**	0.657	87.5%	76.7%	82.1%	75.0%	88.5%	<0.001

*ROC analyses were used.

Table 3

AUC values of the ROC analyses with their 95% confidence intervals (CIs) and standard errors (SEs) using *D*, β, μ, and combination of *D* and β for differentiating low- (positive) from high-grade (negative) gliomas.

	AUC	95% CI of AUC*	SE**
D	0.781	0.647 to 0.882	0.0633
β	0.853	0.730 to 0.934	0.0511
μ	0.703	0.563 to 0.819	0.0736
***D*+ β**	0.853	0.730 to 0.934	0.0511

*Binomial exact Cis.

**SEs were computed by the method of DeLong et al.[46] using MedCalc.